

**Supplemental information: Ultrasound-based formation of nano-Pickering emulsions investigated via in-situ SAXS**

Yi-Ting Lee<sup>[1] §</sup>, David S. Li<sup>[1, 2] §</sup>, Jan Ilavsky<sup>[3]</sup>, Ivan Kuzmenko<sup>[3]</sup>, Geng-Shi Jeng<sup>[2]</sup>, Matthew O'Donnell<sup>[2]</sup>, and Lilo D. Pozzo<sup>[1]\*</sup>

[1] Department of Chemical Engineering, University of Washington, Seattle, WA, USA

[2] Department of Bioengineering, University of Washington, Seattle, WA, USA

[3] X-Ray Science Division, Argonne National Laboratory, Argonne, IL, USA

§These authors contributed equally to this work

\*E-mail: dpozzo@uw.edu

\*Phone: 1-206-685-8536

*Energy barrier calculations*

The interaction potential between a polymer coated particle and emulsion surface was calculated using the Dolan Edwards model.<sup>1,2</sup> Theoretical interaction energy potential between a 12 nanometer diameter particle coated with a 10 kDa molecular weight PEG-thiol and non-polymer coated emulsion droplet was estimated using equations (1) and (2). This estimation showed that there was a significant energy barrier (relative to kT) between the two surfaces. Thus, it was not possible to induce spontaneous adsorption and would require a large force into the system to form Pickering emulsions.

$$d_{modified} < \sqrt{3} \times R_F: \frac{E(d)}{kT} = \Gamma \left\{ \ln \left[ \left( \frac{d^2}{8\pi lL} \right)^{0.5} \right] + \frac{\pi^2}{2} \left( \frac{lL}{d^2} \right) \right\} \quad (1)$$

$$d_{modified} > \sqrt{3} \times R_F: \frac{E(d)}{kT} = -\Gamma * \ln \left\{ 1 - 2 \times \exp \left[ \frac{-d^2}{2lL} \right] \right\} \quad (2)$$

where:

- d: Separation distance
- $R_F$ : Flory radius of the polymer chain
- k: Boltzmann constant
- T: Temperature
- l: Length of monomer in the polymer chain
- L: Contour length of the polymer chain
- $\Gamma$ : Surface density of the anchored polymer chain

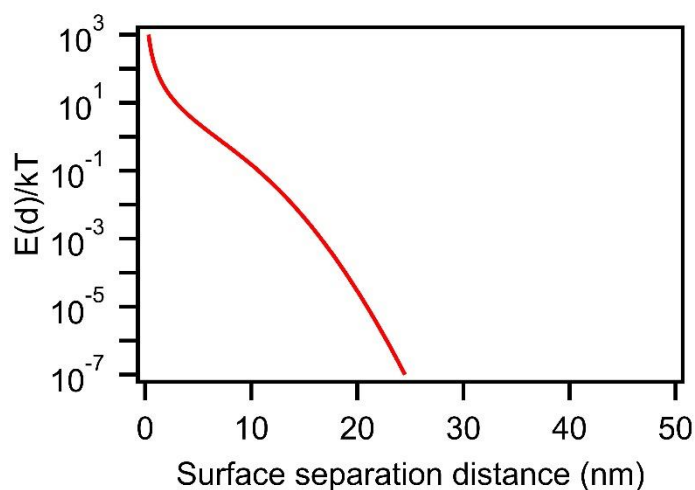


Figure S1. Theoretical estimation of energy barrier between a polymer grafted nanoparticle and emulsion surface using the Dolan Edwards model where  $R_F = 6.0$  nm,  $l = 0.3$  nm,  $L = 63.0$  nm, and  $\Gamma = 1.2$  chains/nm<sup>2</sup>.

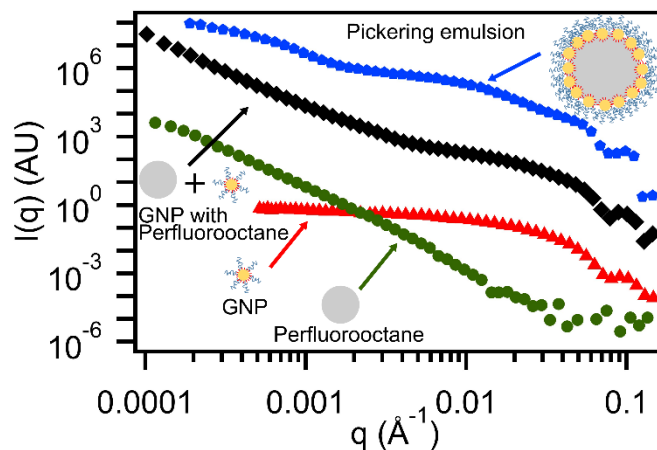
### Optimizing hydrophobic vs hydrophilic forces on synthesized GNP

To effectively examine the role of sonication during emulsion formation, it was crucial to choose the correct type and amount of hydrophilic/hydrophobic chains used to functionalize GNPs. Based on previous experiences, increasing the grafting densities or using larger molecular weights of the dosed hydrophilic PEG-thiol to functionalize the surface of GNPs increases the stability of the particles and results in smaller nanoclusters.<sup>3</sup> If the additional steric repulsion force on GNPs is strong enough to overcome the hydrophobic attractive force, the GNPs will stay as a stable ‘singlet’ spherical particles and will not form larger structures. These stable GNPs have been shown to stay in this ‘singlet’ form even after sonication.

Selecting the right hydrophobic alkane thiol was also important. For these experiments, we selected the smallest amounts needed to fully coat the surface of the GNPs, avoiding a large excess of thiol. We also selected to use shorter thiol chains that have been shown to form more surface active particles and lead to more pronounced correlation peaks in the scattering profiles from Pickering emulsions.<sup>4</sup> If the spacing between gold nanoparticles at the emulsion interface is limited by the length of the alkane thiol (i.e. assuming close contact), then the use of short chain alkane thiols can result in denser packing of nanoparticles on a finite emulsion interface. More particles on the emulsion would then result in more particle-particle correlations and a more pronounced characteristic peak in the mid-q regions of the scattering profiles. For a 12 nm diameter butanethiol functionalized GNP, the theoretical maximum surface coverage estimated was around 82% whereas longer chains such as octanethiol had a theoretical maximum surface coverage of 67%.<sup>5</sup>

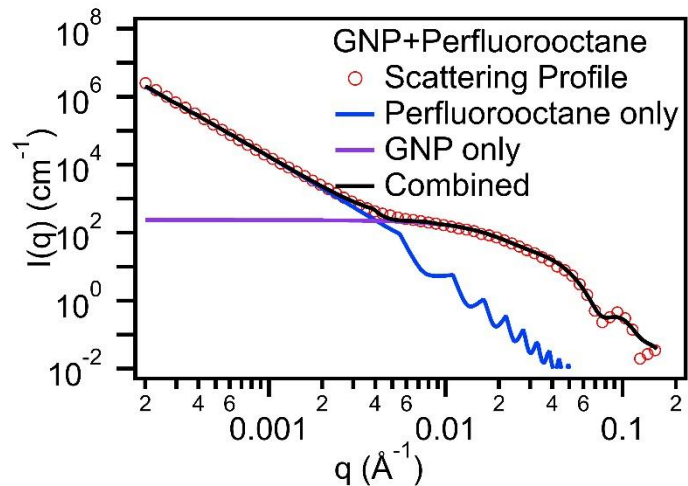
*Ultra-small X-ray scattering profile of different components in the Pickering emulsion synthesis process*

An example of the scattering profile of the different materials used for our Pickering emulsion synthesis is shown in figure S2. As can be seen, emulsions had higher scattering intensities in the lower q region whereas GNP dominated the scattering intensities at high q regions. When the two materials were combined, scattering data were basically a combination of the two different components. However, when sonicated at high acoustic pressure, the scattering profile of the sample significantly alters in the mid and low q regions indicating the formation of Pickering emulsions.



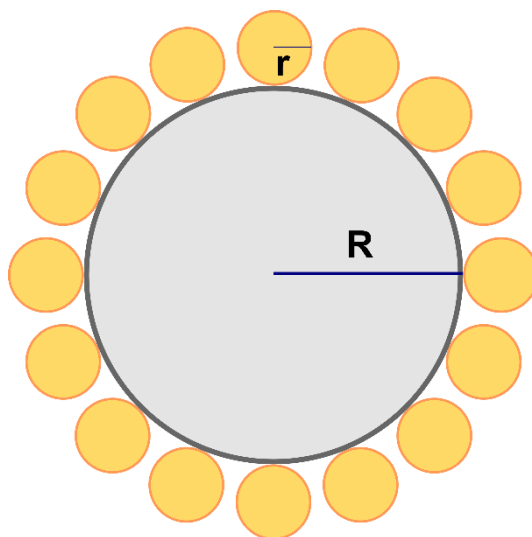
**Figure S2.** Example of desmeared USAXS data for **perfluorooctane** emulsions, GNP, GNP with **perfluorooctane** emulsions presence (no sonication), and Pickering emulsions. Scattering data are arbitrarily shifted in the y axis to show the difference in the characteristic between curves.

Figure S3 is an example of modeling the scattering profile of a sample sonicated at low acoustic pressure showing that the final fitted scattering curve was a combination of two spheres, one for emulsions and one for gold nanoparticles. Fits suggest that the system consisted of a polydisperse **perfluorooctane** with mean radius of 411.6 nanometers with a PDI of 0.5. In addition, two different size distributions of GNPs were present, where 78.5 vol% of the particles had a radius of 6.00 nm and 21.5 vol% were 13.3 nm. This model was also used to provide information on the changes of emulsion droplet size and volume fraction in the sample during sonication.



**Figure S3.** Desmeared USAXS scattering data at low acoustic pressure can be fitted with a model containing 2 spherical components, the **perfluorooctane** emulsion and GNP.

*Debye model formulas and validation of the model*



**Figure S4.** Schematic figure of a Debye model used to fit Pickering emulsion scattering data. A spherical emulsion droplet with a radius  $R$  is evenly coated by  $N$  spherical GNPs with a radius  $r$ .

A Debye model consisting of N smaller spheres (GNP) surrounding a large sphere (emulsion) was used to represent synthesized Pickering emulsions. All spheres were assumed to be hard spheres; therefore, they would not overlap with each other. The schematic of the Pickering emulsion is shown in figure S4. The scattering intensity of a Pickering emulsion was divided into multiple terms, including scattering intensity of the individual GNPs, emulsion droplets, scattering due to the interactions between GNPs vs the emulsion droplets, and GNP-GNP interactions. Since both GNPs and emulsions in the system were all spheres, their form factors were expressed as the following equations, where q is the scattering vector, r and R are the radii of the GNPs and emulsion droplets, and  $\rho$  the scattering length density of the components or water.

$$F_{particle} = (\rho_p - \rho_{solvent})V_p \frac{3[\sin(qr) - qr \cos(qr)]}{(qr)^3} \quad (3)$$

$$F_{oil} = (\rho_o - \rho_{solvent})V_o \frac{3[\sin(qR) - qR \cos(qR)]}{(qR)^3} \quad (4)$$

$$V_p = \frac{4}{3}\pi r^3 \quad (5)$$

$$V_o = \frac{4}{3}\pi R^3 \quad (6)$$

The scattering intensities of the individual components and the interactions between these components was then calculated using equations 7 through 10.

$$P_{particle} = (F_{particle})^2 \quad (7)$$

$$P_{oil} = (F_{oil})^2 \quad (8)$$

$$P_{op} = 2NF_{oil}F_{particle} \frac{\sin(q(R+r))}{q(R+r)} \quad (9)$$

$$P_{pp} = 2(F_{particle})^2 \sum_{i=1}^{N-1} \sum_{j=i+1}^N \frac{\sin[q(\hat{r}_i - \hat{r}_j)]}{q(\hat{r}_i - \hat{r}_j)} \quad (10)$$

The scattering intensity of one Pickering emulsion was then expressed as the summation of all the individual components with a weighing factor, where  $\rho_o$  is the scattering length density (SLD) of the emulsion core,  $\rho_{solvent}$  is the SLD of the solvent, and  $\rho_{particle}$  is the SLD of the gold nanoparticles

$$P_{Pickering} = \frac{1}{M^2} (P_{particle} + P_{oil} + P_{op} + P_{pp}) \quad (11)$$

$$M = (\rho_o - \rho_{solvent})V_o + N(\rho_p - \rho_{solvent})V_p \quad (12)$$

However, since there were some particles not bound to the emulsion interface and free floating in the system, the final scattering intensity of a monodisperse Pickering emulsion with some excess particle in the system was then expressed as the following equation, where  $\phi_o$  is the volume fraction of the oil phase,  $\phi_p^{total}$  is the dosed total volume fraction of the particles, and  $\phi_{ex}$  is the estimated ratio of excess particles in the system.

$$I_{sys} = [\phi_o(\rho_o - \rho_{solvent})V_o + \phi_p^{total}(1 - \phi_{ex})N(\rho_p - \rho_{solvent})V_p]P_{Pickering} + \phi_p^{total}\phi_{ex}\frac{P_{particle}}{V_p} \quad (13)$$

Polydispersity of the Pickering emulsions was included by assuming their size distribution to be lognormal. The probability of each size within a bin size was estimated using the standard normal table on a log scale. Using more bins to express the lognormal distribution would provide a better estimation of the distribution but the scattering intensity calculation time also significantly

increases with the increasing number of bins; therefore, a total of 5 bins was used for all modeling results shown in this report.

The model was verified by changing the parameters and observing how scattering intensity characteristics varied. To simplify the system, a model where there were only Pickering emulsions and no 'free' excess particles was first examined to determine which parameters had the most effect on the scattering curve (figure S5). Parameters including Pickering emulsion radius, amount of emulsion surface covered, and emulsion polydispersity were then varied while other parameters were kept constant. Based on the modeling results, increasing the Pickering emulsion radius resulted in a shift of the Guinier region into lower  $q$ . Increasing emulsion surface coverage gave rise to a shift of the characteristic peak, the GNP-GNP interaction peak, into higher  $q$  regions. And finally increasing the polydispersity of the emulsion droplet smoothed the scattering curve.



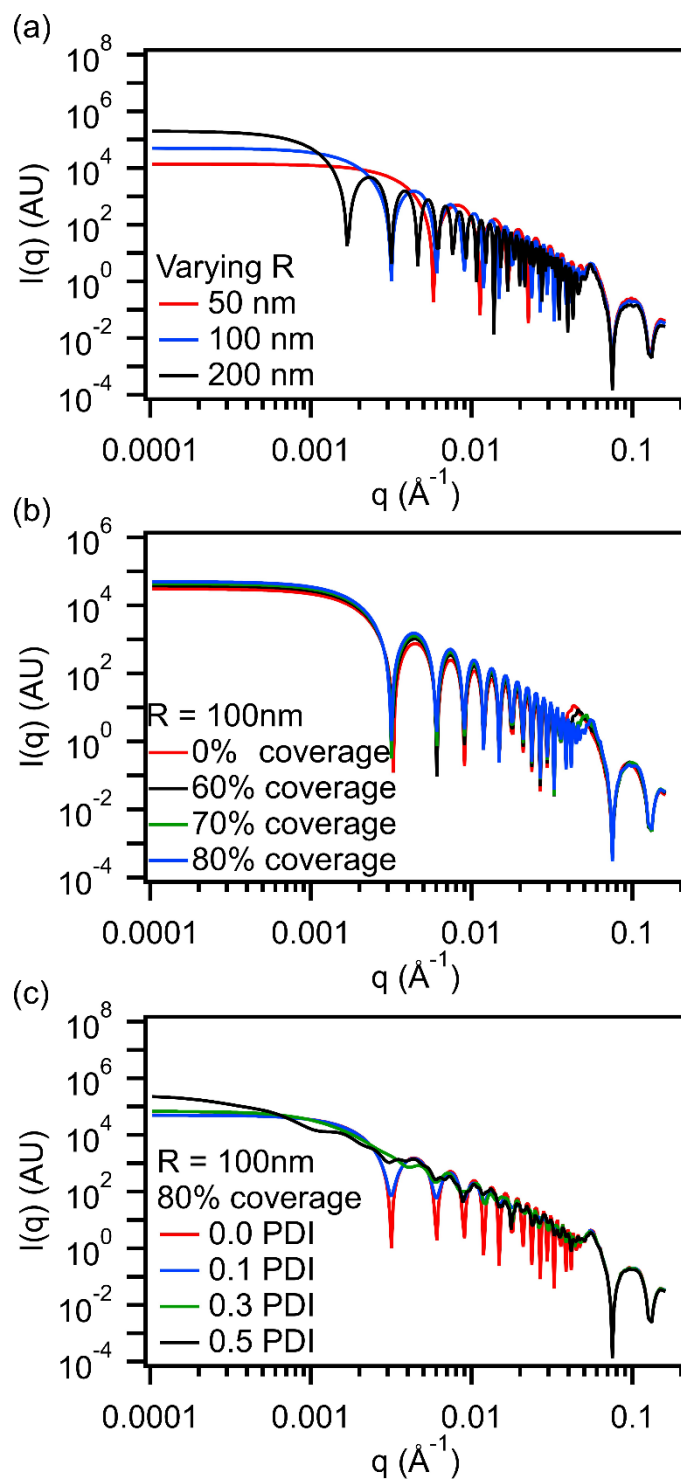
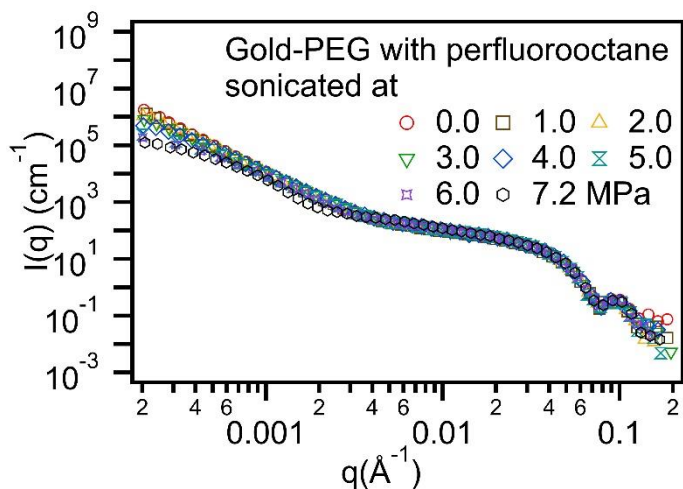


Figure S5. Debye model of Pickering emulsions varying emulsion (a) radius, (b) surface coverage, and (c) polydispersity. No instrumental smearing or polydispersity is included in these models. Scattering length densities were fixed for water ( $9.47 \times 10^{-6} \text{\AA}^{-2}$ ), gold ( $124.69 \times 10^{-6} \text{\AA}^{-2}$ ) and emulsion ( $14.47 \times 10^{-6} \text{\AA}^{-2}$ ).

### Control samples to help determine Pickering emulsion formation

To investigate the role of sonication in the formation of Pickering emulsions, it was important to be sure that no false positives were observed during experiments. The first control experiment used hydrophilic gold nanoparticles (Gold-PEG) with emulsion droplets to determine whether or not Pickering emulsions could be synthesized without hydrophobic alkane thiol chains. Figure S6 is an example of the result of scattering data obtained showing no Pickering emulsion characteristic peaks were formed in the mid  $q$  region regardless of the acoustic pressure. The only difference was the change in slope in the low  $q$  regions suggesting that the only change in the system was the size distribution of emulsion droplets.



**Figure S6.** USAXS profile for Gold-PEG with perfluorooctane sonicated at different acoustic pressure showing that Gold-PEG will not adsorb onto emulsion surfaces even when sonicated at high acoustic pressures.

GNP alone was also evaluated to determine whether or not it would form a larger structure when sonicated. As mentioned in the discussion, choosing the correct parameters for synthesizing

GNPs was crucial. Figure S7, the result of sonicating GNPs alone, showed that no larger clusters were formed even when with cavitation. These two control experiments proved that it was safe to assume that any significant changes observed in the scattering profile when sonicating a GNP with emulsion sample was from formation of Pickering emulsions.

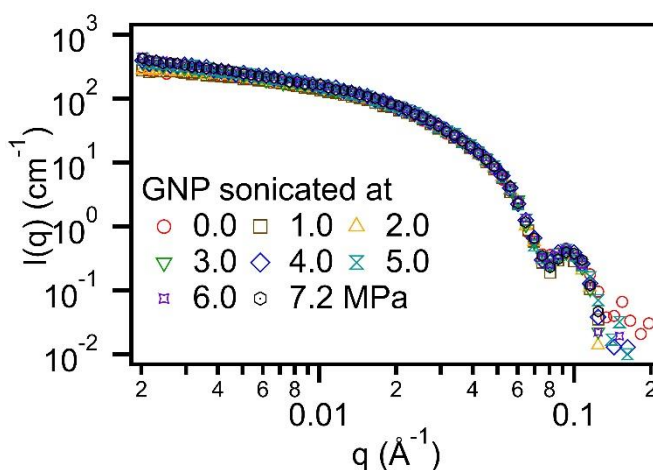


Figure S7. USAXS profile of GNP sonicated at different acoustic pressure showing that no larger structures will form even with cavitation.

#### Using FTIR spectrum to verify the integrity of the ligands on the GNPs

Fourier-transform infrared spectroscopy (FTIR) was performed on GNP with perfluorooctane samples before and after sonication. The samples were synthesized, lyophilized, mixed with dry KBr and pressed into a pellet using KBr pellet a die kit. The FTIR measurements were performed using a Bruker Vector 33 FTIR spectrophotometer (Bruker Corporation, MA, USA). This experiment was used to examine whether or not cavitation events have an effect on the ligands binding to the GNP surfaces. The obtained spectra are shown in figure S8. The broad peak in the  $3100\text{-}3700 \text{ cm}^{-1}$  region corresponds to the OH group on the PEG-thiol. The peak at around  $1100 \text{ cm}^{-1}$  is from the C-O bond on the PEG-thiol and the peak in the  $2800\text{-}2950 \text{ cm}^{-1}$  region is from the alkane bonds (combination of PEG-thiol and alkanethiol). The presence of a

peak at  $2350\text{ cm}^{-1}$  is due to  $\text{CO}_2$ , which was a small background subtraction error within the instrument. Since the FTIR spectrum of the sample before and after sonication remains identical, it demonstrates that alkanethiol and PEG-thiol coatings are unaffected by the application of ultrasound.

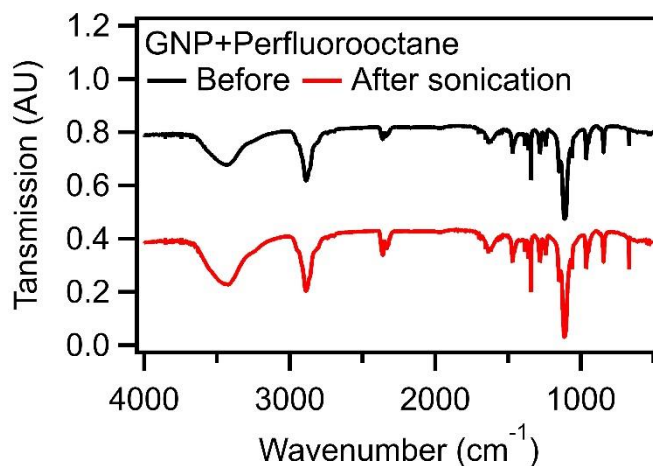


Figure S8. FTIR spectrum of GNP with perfluorooctane before and after sonication.

#### **Supplemental references:**

- (1) Dolan, A. K.; Edwards, S. F. *Proc. R. Soc. A Math. Phys. Eng. Sci.* **1974**, 337 (1611), 509–516.
- (2) Li, F.; Pincet, F. *Langmuir* **2007**, 23 (25), 12541–12548.
- (3) Larson-Smith, K.; Pozzo, D. C. *Soft Matter* **2011**, 7 (11), 5339–5347.
- (4) Larson-Smith, K.; Pozzo, D. C. *Langmuir* **2012**, 28 (32), 11725–11732.
- (5) Porter, M. D.; Bright, T. B.; Allara, D. L.; Chidsey, C. E. *J. Am. Chem. Soc.* **1987**, 109 (12), 3559–3568.